Progress in High Temperature Oxidation Modeling: Internal and External Oxidation

Youhai Wen, Tianle Cheng, Jeffrey Hawk, David Alman

Research & Innovation Center, NETL

U.S. DEPARTMENT OF ENERGY | National Energy Technology Laboratory

CROSSCUTTING RESARCH REVIEW MEETING, APR 18-22, 2016, PITTSBURGH, PA

Acknowledgements

- **Technology Development & Integration Center, NETL, for supporting this Research & Innovation Center (RIC) activity through Innovative Process Technologies (IPT) Field Work Proposal.**

  Robert Romanosky Charles Miller Vito Cedro Karol Schrems

- John Baltrus (NETL)
- Helpful discussions with Gordon Holcomb (NETL) & Brian Gleeson’s group member (U. Pitt)

IPT Task 3.4: Computational Aspects in Alloy Design & Life Prediction

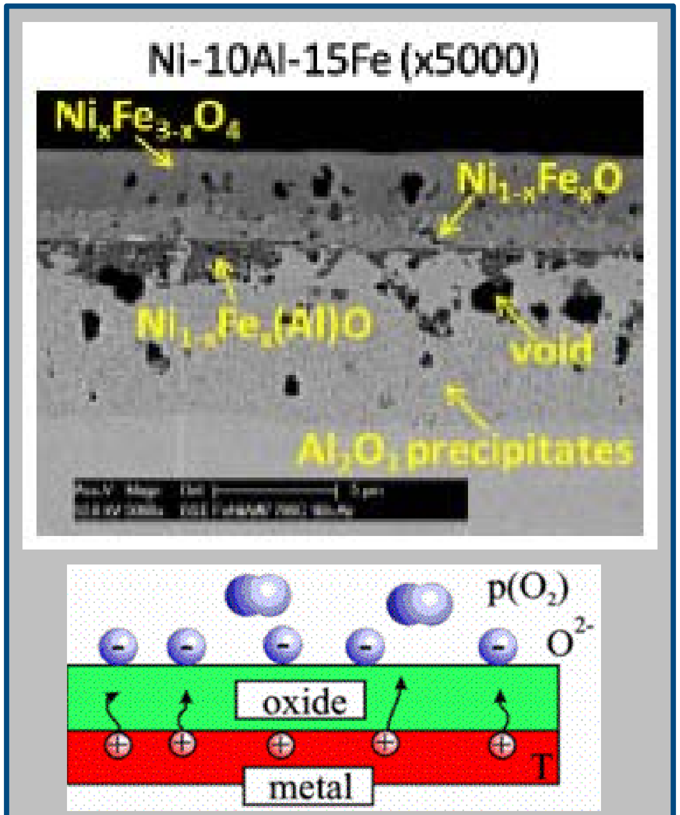

Metal Oxidation

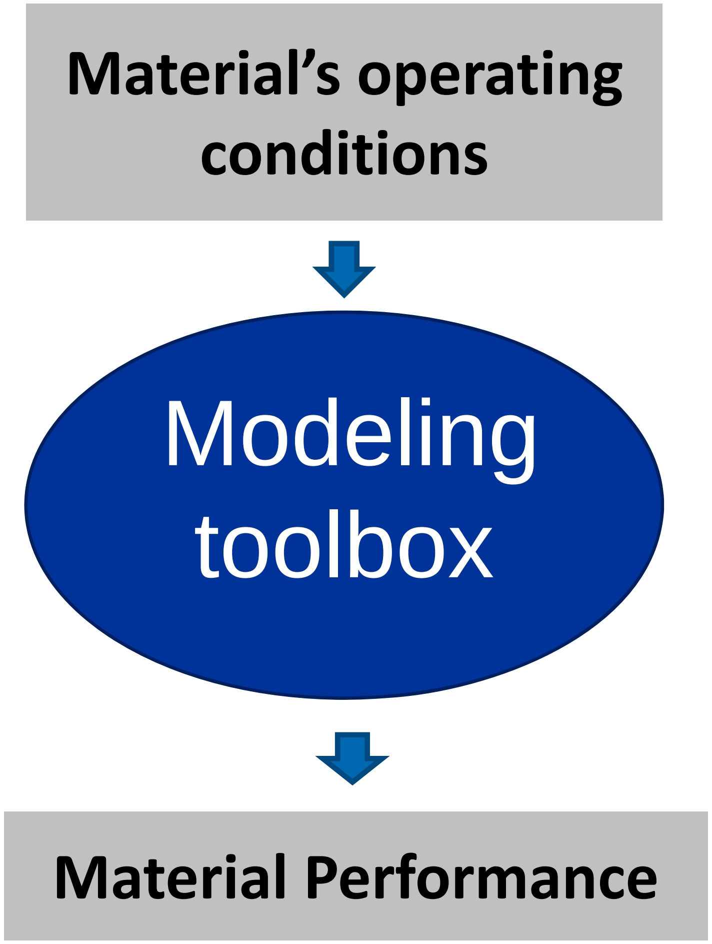

Material's operating conditions

Modeling toolbox

Material Performance

(Source: Internet)

Metal Oxidation Modeling

State-of-the-art of Computational Modeling

Cabrera -Mott Theory

Moderate film thickness

Wagner Theory

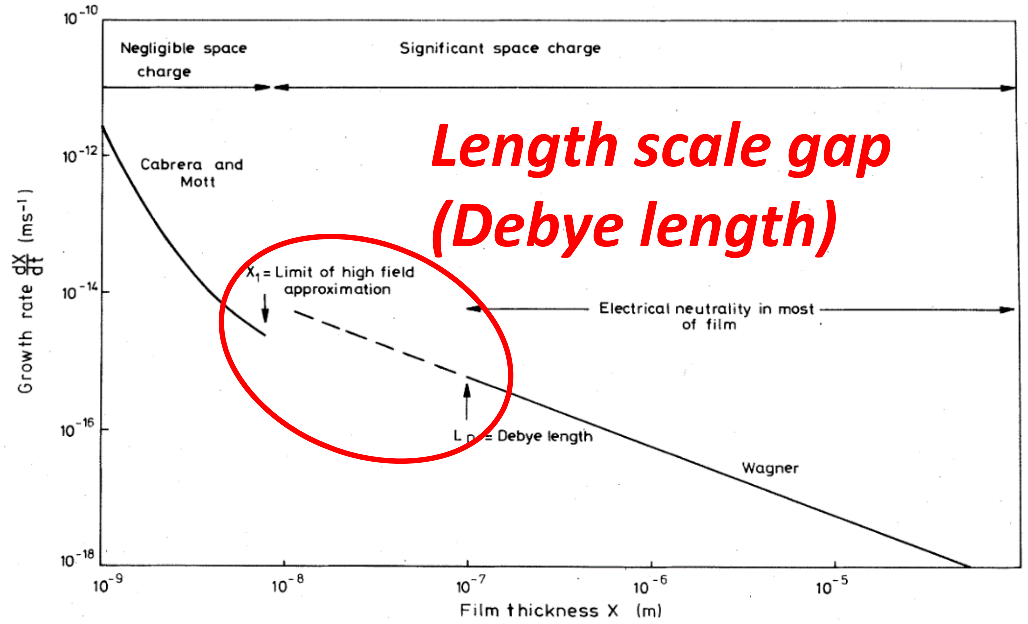

Length scale gap (Debye length)

(Atkinson, *Review of Modern Physics*, 1985)

In this intermediate length regime, some common simplifications are not applicable such as local charge neutrality or constant electric field.

Length Scale Gaps in Oxidation Theories

Cabrera -Mott Theory

Moderate film thickness

Wagner Theory

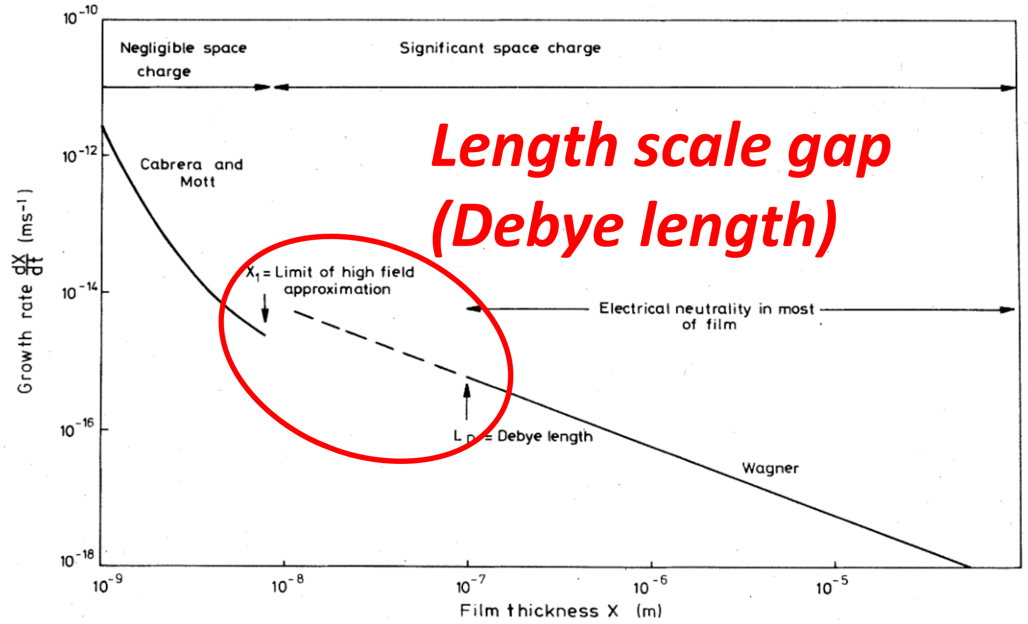

Length scale gap (Debye length)

(Atkinson, *Review of Modern Physics*, 1985)

Moderate film thickness regime: *The coupling of charge interaction, ionic diffusion, and chemical reaction have to be addressed.*

Oxidation Modeling in Pure Metals

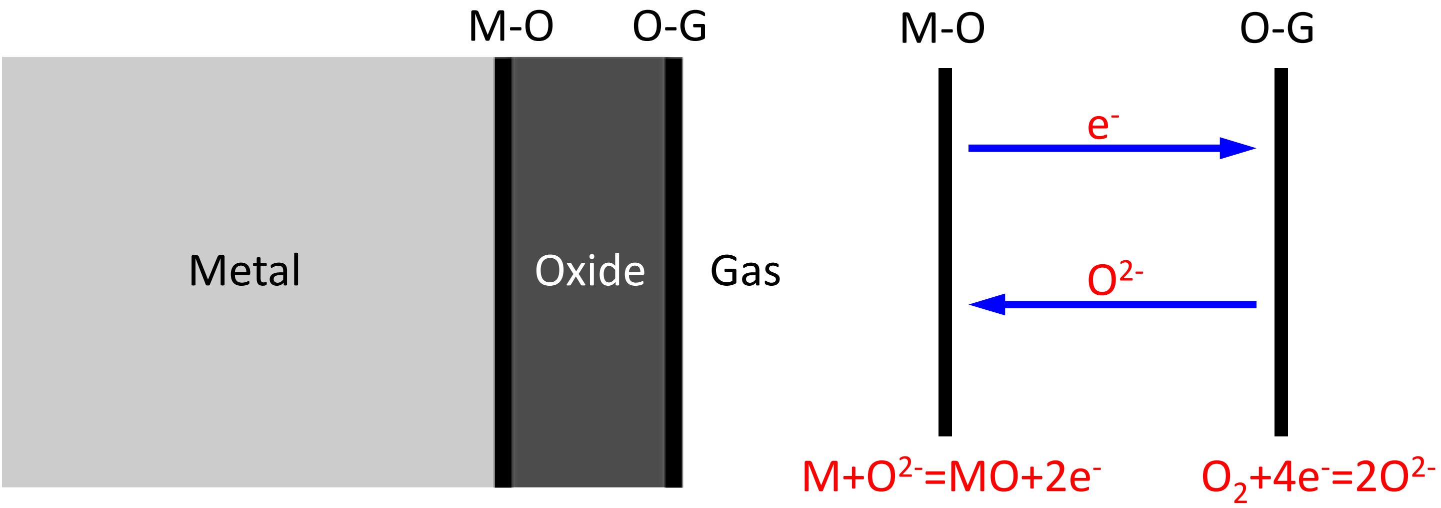

$M+O^{2-}=MO+2e^-$ $O_2+4e^-=2O^{2-}$

Coupling physics with no viable simplification

- **Chemical reaction**
- **Mass transport**
- **Charge interaction**
- **Evolving structure**
- **Evolving electric field**

Phase-field Method

Governing Equations for Metal Oxidation

Reaction

Diffusion + Electromigration

$$
\begin{aligned}
&[X^-]: && \frac{\partial c_1}{\partial t} = K_I \Lambda_\zeta (Q\tilde{c}_2 - \tilde{c}_1) - K_{II}\Lambda_\eta \tilde{c}_1 + \nabla\cdot(\tilde{D}_1 \nabla \tilde{c}_1) - \frac{e}{k_B T}\nabla\cdot(D_1 c_1 z_1 \mathbf{E}) \\
&[e^-]: && \frac{\partial c_2}{\partial t} = -K_I \Lambda_\zeta (Q\tilde{c}_2 - \tilde{c}_1) + K_{II}\Lambda_\eta \tilde{c}_1 + \nabla\cdot(\tilde{D}_2 \nabla \tilde{c}_2) - \frac{e}{k_B T}\nabla\cdot(D_2 c_2 z_2 \mathbf{E}) \\
&[c^+]: && \frac{\partial c_3}{\partial t} = \nabla\cdot(D_3 \nabla c_3) - \frac{e}{k_B T}\nabla\cdot(D_3 c_3 z_3 \mathbf{E}) \\
&[M]: && \frac{\partial \eta}{\partial t} = -K_V K_{II}\Lambda_\eta \tilde{c}_1 + M_\eta \nabla^2\left(\partial f / \partial \eta - \beta \nabla^2 \eta\right)
\end{aligned}
$$

The electric field, satisfying Poisson's equation, is solved by **an efficient numerical scheme** for arbitrary **dielectric heterogeneity**

$$
\boxed{\nabla\cdot[\varepsilon(\mathbf{r})\nabla\varphi(\mathbf{r})] + \rho_f(\mathbf{r}) = 0}
$$

Simulated Results on Oxidation Kinetics Modeling

Linear → Parabolic kinetics Transition

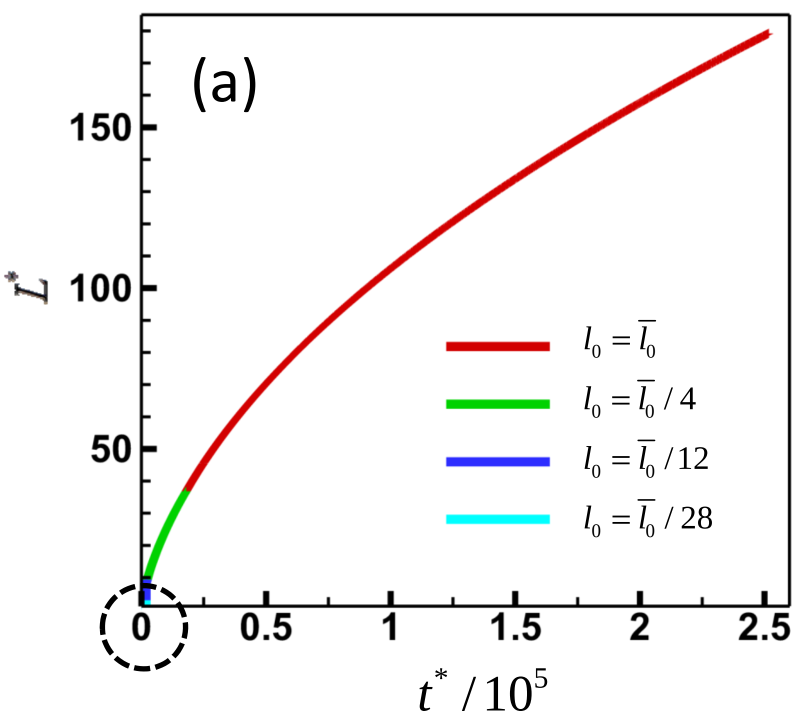

Overall growth kinetics

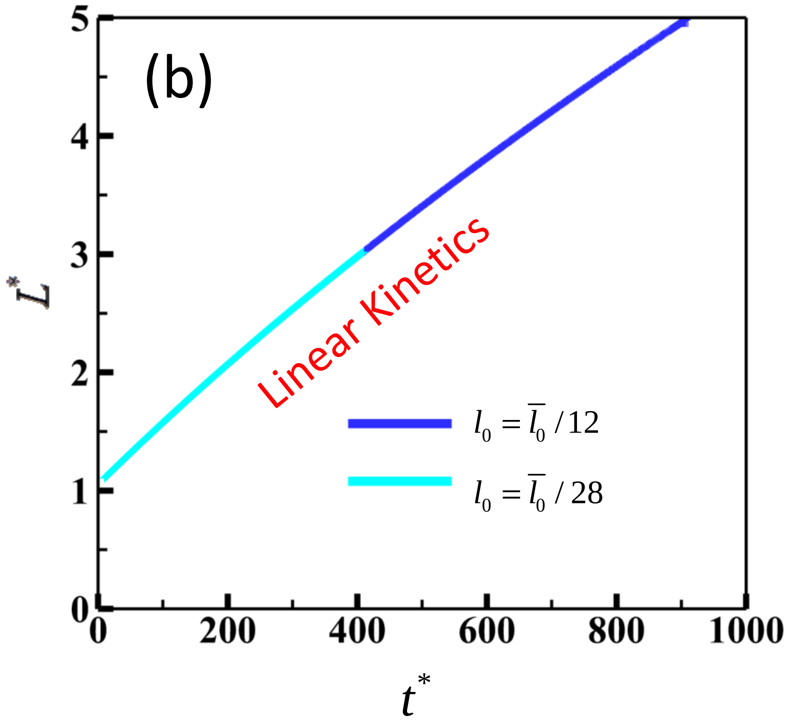

Initial stage growth kinetics

T Cheng, Y Wen and J Hawk, J. Phys. Chem. C 118(2014), 1269-1284

Oxide Growth Rate vs. Film Thickness

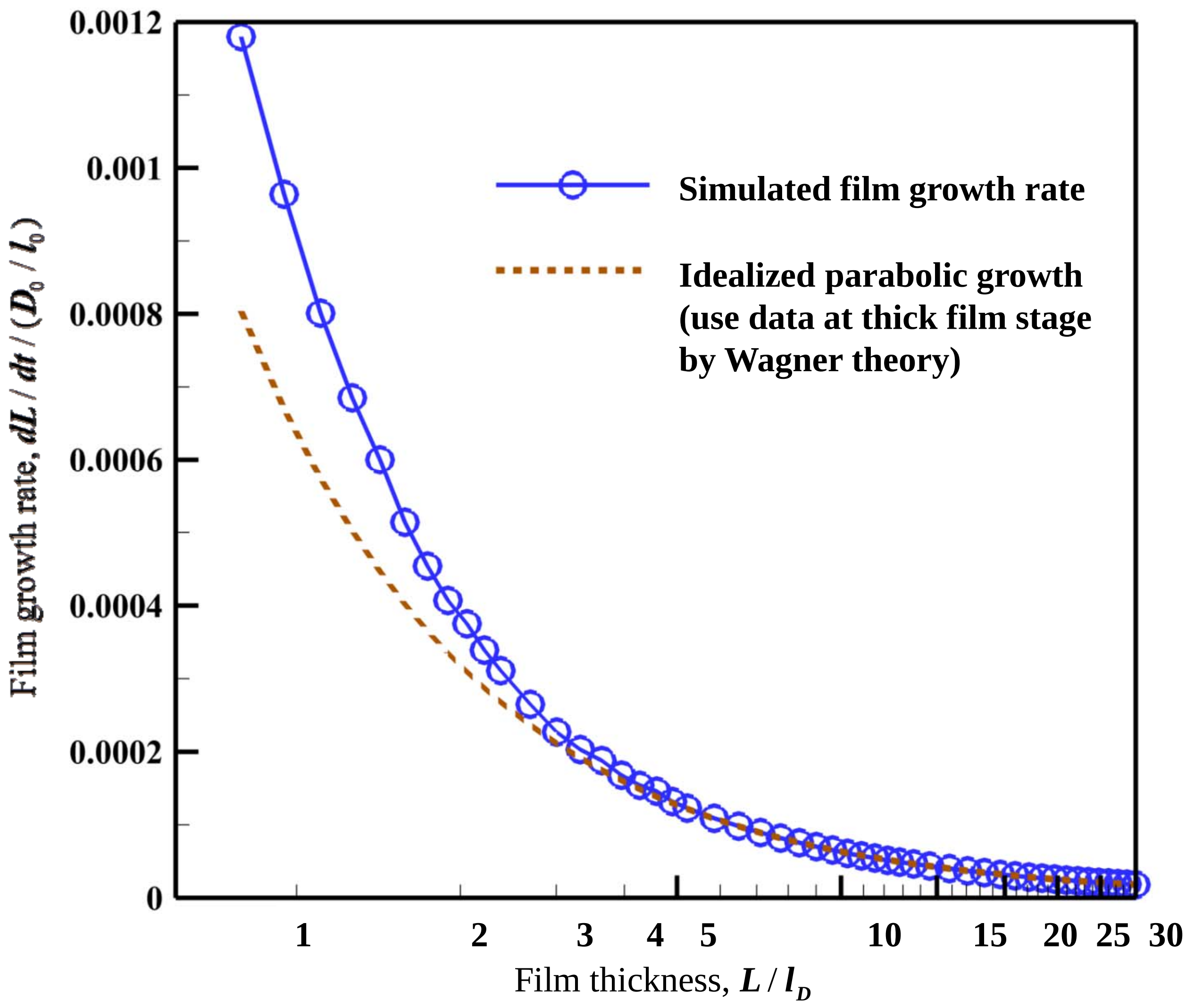

Space charge effect can not be ignored

Summary

Physics-based Modeling Capability on **External Oxidation** so far …

Modeling Internal Oxidation

Why we care?

- Oxidation usually starts with internal selective oxidation of certain solute elements
- Transition from internal to external oxidation is the basis for alloy design regarding oxidation resistance.

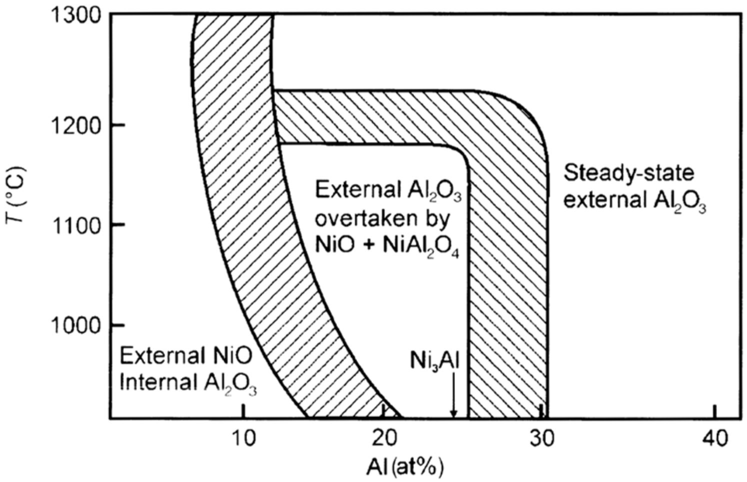

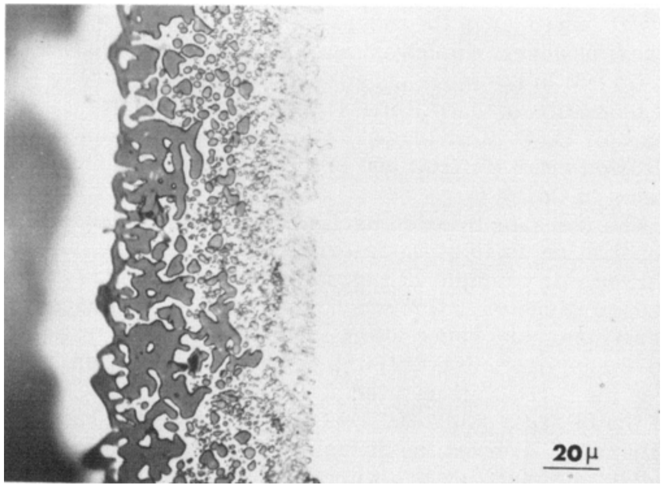

Oxidation Map: Compositional effects on the oxidation of Ni-Al alloys

(N. Birks, G. Meier, F. Pettit, 2006)

Transition from internal to external oxidation in Co-8.99%Ti: 900˚C for 528h

(J. Megusar; G. Meier, 1976)

Modeling Internal Oxidation

State-of-the-art about theoretical understanding

- **Analyzed by C. Wagner in 1959 for a binary system with 1D assumption – Oversimplification!**
- **Remains an open problem especially in consideration of the complex microstructure in 3D situations**

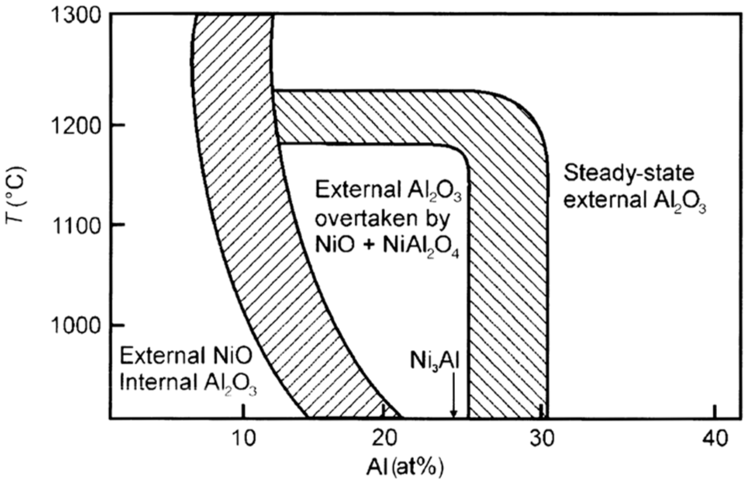

Oxidation Map: Compositional effects on the oxidation of Ni-Al alloys (N. Birks, G. Meier, F. Pettit, 2006)

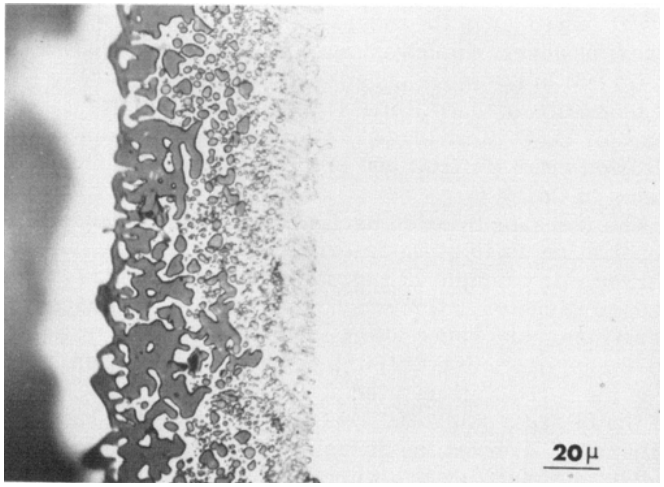

Transition from internal to external oxidation in Co-8.99%Ti at 900˚C for 528h,
(J. Megusar; G. Meier, 1976)

Wagner's theory on the transition from internal to external oxidation

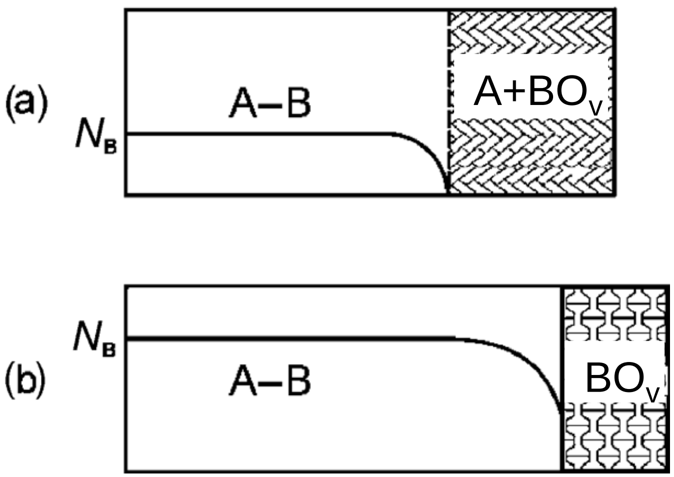

Transition criterion (C. Wagner 1959):

$$N_B^{(O)} > \left[\frac{\pi f^*}{2\nu} \frac{V_m}{V_{ox}} \frac{D_O N_O^{(S)}}{D_B} \right]^{1/2}$$

Schematic: transition from internal to external oxidation of solute B to the formation of an external layer of BO$_v$.
(a) internal oxidation,
(b) external oxidation with higher C_B
(after N. Birks, G. Meier, F. Pettit, 2006)

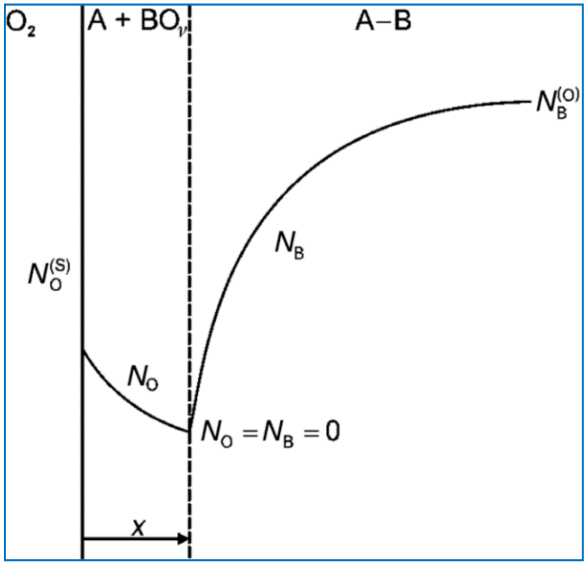

Schematic: Concentration profiles for internal oxidation of A-B (Birks, Meier, Pettit, 2006)

Wagner's theory on the transition from internal to external oxidation

Transition criterion (C. Wagner 1959):

$$N_B^{(O)} > \left[\frac{\pi f^*}{2\nu} \frac{V_m}{V_{ox}} \frac{D_O N_O^{(S)}}{D_B} \right]^{1/2}$$

$f^* = 0.3$ (for Ag-In system) (R. A. Rapp, 1961)

$f^* \sim 0.5$ (for Fe-Si system) (W. Zhao, Y. Kang, J. Orozco, B. Gleeson, 2015)

There is no universal/general f^* even just for binary systems!

No Predication Capability!

Phase-Field Modeling of Internal Oxidation

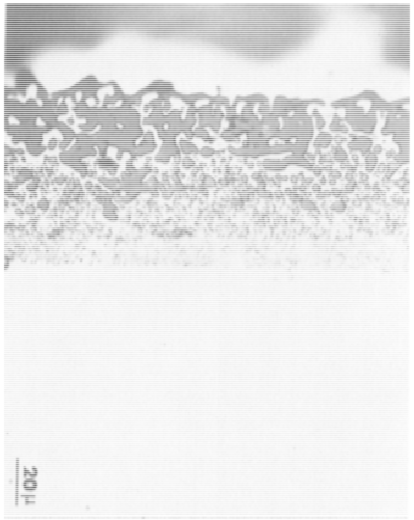

Co-8.99%Ti oxidized at 900˚C for 528h,
(J. Megusar; G. Meier, 1976)

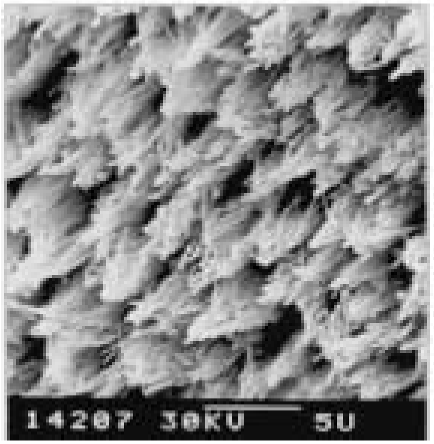

Ni-8.67Al oxidized at 1000˚C (after deep etching) (A. M.-Villafane, F. Stott, J. C.-Nava, G. Wood, 2002)

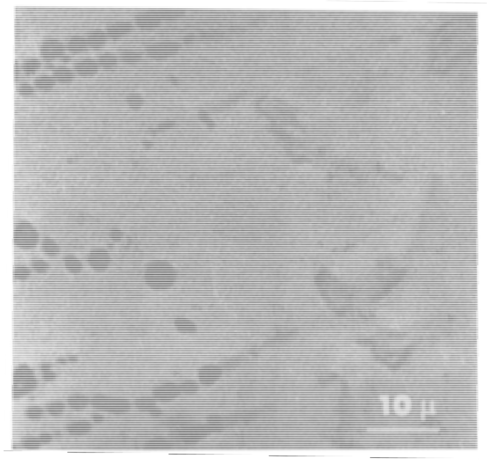

TiO_2 needles in Co-3.7Ti alloys after reaction front passed.
(J. Megusar and G. Meier, 1976)

Microstructure evolution in internal oxidation can be very different depending on specific material systems and it is no surprise that the critical volume fraction for the transition from internal to external oxidation is not a constant

Technical Challenges #I

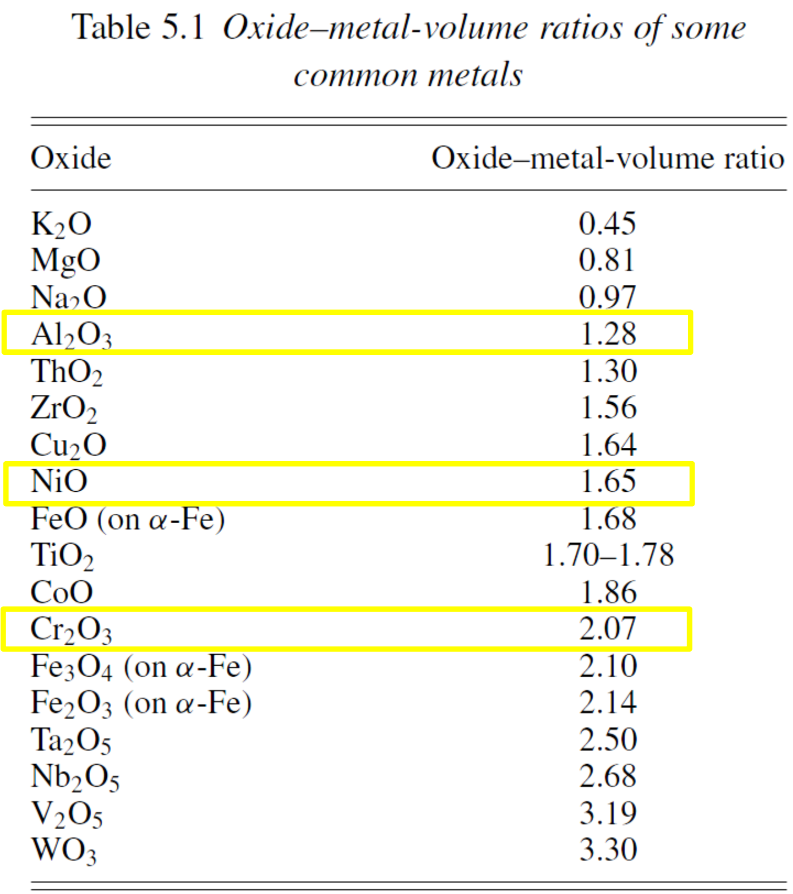

Table 5.1 *Oxide–metal-volume ratios of some common metals*

Oxide	Oxide–metal-volume ratio
K_2O	0.45
MgO	0.81
Na_2O	0.97
Al_2O_3	1.28
ThO_2	1.30
ZrO_2	1.56
Cu_2O	1.64
NiO	1.65
FeO (on α-Fe)	1.68
TiO_2	1.70–1.78
CoO	1.86
Cr_2O_3	2.07
Fe_3O_4 (on α-Fe)	2.10
Fe_2O_3 (on α-Fe)	2.14
Ta_2O_5	2.50
Nb_2O_5	2.68
V_2O_5	3.19
WO_3	3.30

(Hancock and Hurst, 1974)

Plastic deformation with oxide growth quite common

- relieves elastic strain energy (oxide morphology evolution)
- may be time dependent (viscoplasticity)

Need to Develop a Plastic and Viscoplastic Deformation Modeling Capability!

Technical Challenges #II

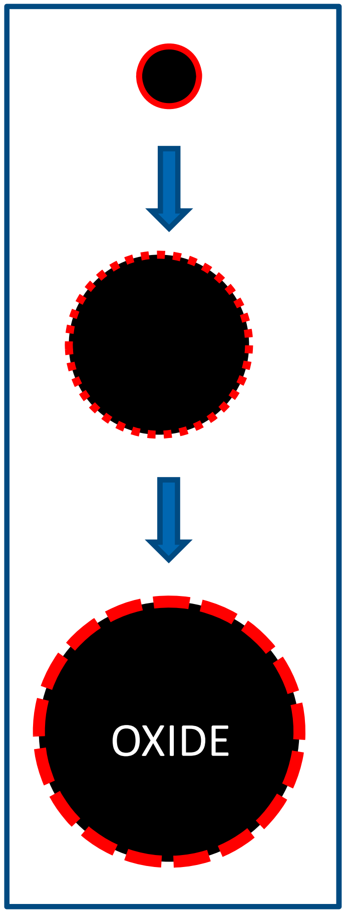

Interface Coherence
with Oxide Growth

Oxide-matrix interface:

- typically coherent for small precipitates
- Loses coherency upon growth

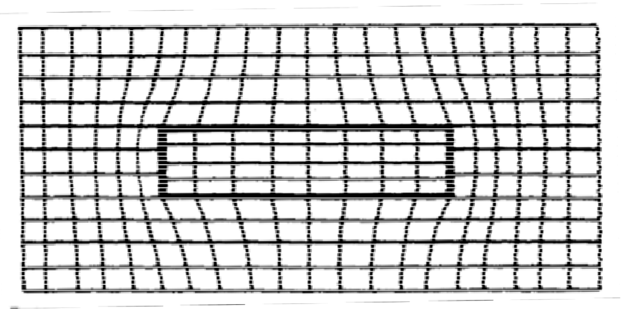

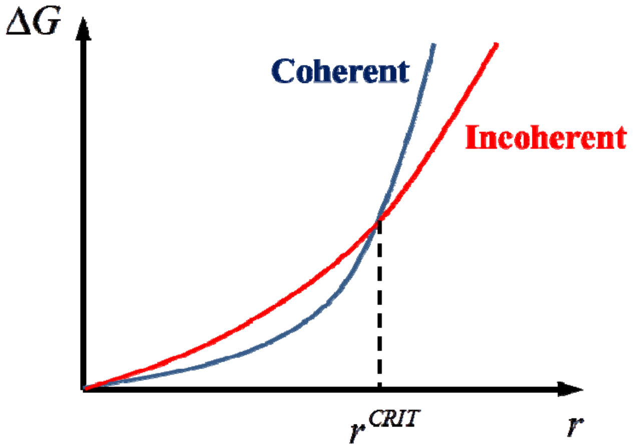

(after D. Porter and K. Easterling, 1996)

$$\Delta G = 4\mu\delta^2 \cdot \frac{4\pi r^3}{3} + 4\pi r^2 \cdot \gamma$$

Technical Challenges #II

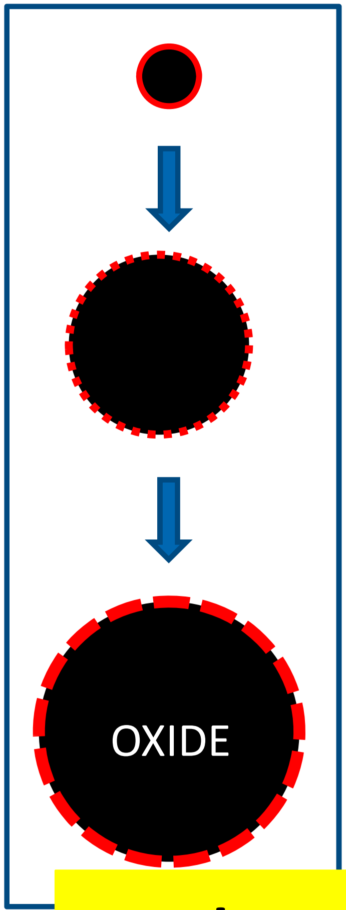

Oxide-matrix interface:

- typically coherent for small precipitates
- Loses coherency

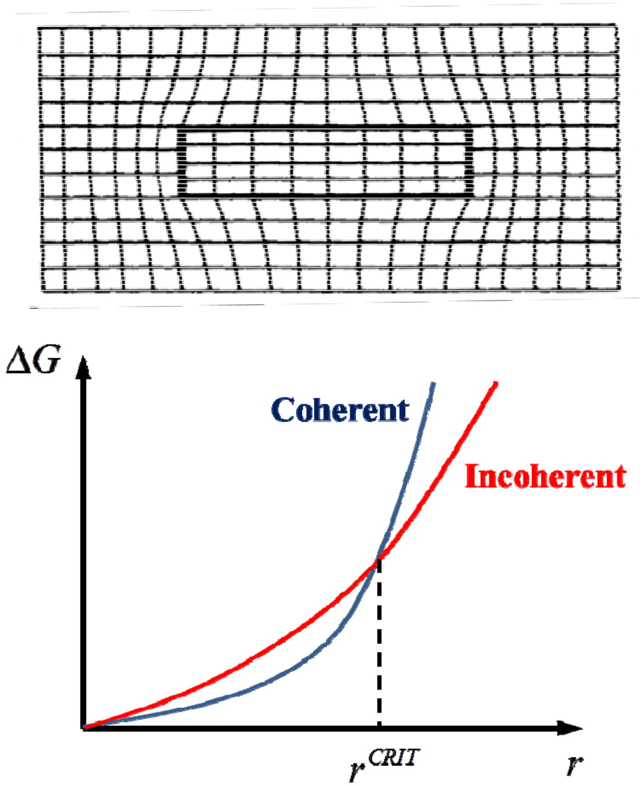

(after D. Porter and K. Easterling, 1996)

Inter

with

Coherency Transition/Loss is Natural & Unavoidable with Oxide Growth!

Technical Challenges #II

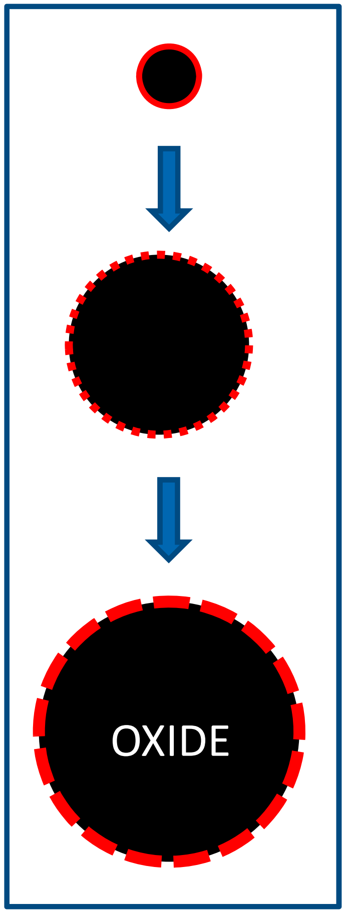

Interface Coherence with Oxide Growth

An incoherent interface typically:

- Higher interfacial energy but lower elastic energy
- No accommodation of shear stress
- Short-circuit diffusion path

Coherency state should have a dominant effect on oxide morphology and growth kinetics!

Coupling between stress and diffusion: affect oxide precipitate morphology & its evolution

Need to develop a comprehensive coherency transition modeling capability!

Outstanding Challenges for Phase-Field Modeling of Internal Oxidation

I. Modeling plasticity due to volume expansion with oxidation

II. Modeling coherency loss involving transition between coherent, semicoherent, and incoherent interfaces

State of the Art

Phase-field models for plasticity:

- Proposed by X. Guo, S. Shi and X. Ma (2005)
  1) Assumed elastic-perfect plasticity – no hardening behavior
  2) Solves plastic strain by calculating the variation of deviatoric strain energy

State of the Art

Phase-field models for plasticity:

- Proposed by X. Guo, S. Shi and X. Ma (2005)
  1) Assumed elastic-perfect plasticity – no hardening behavior
  2) Solves plastic strain by calculating the variation of deviatoric strain energy

Can the deviatoric strain energy be expressed as $E^{dis} = E^{dis}(e_{ij}^{0}, \varepsilon_{ij}^{p})$?

($e_{ij}^{0} = \varepsilon_{ij}^{0} - \varepsilon_{kk}^{0}\delta_{ij}/3$ is the deviatoric part of eigenstrain)

Considering the solution of classical elastic inclusion problem by Eshelby, for a spherical inclusion with dilatational eigenstrain

$$\varepsilon_r = \varepsilon_t = \frac{1}{3}\frac{1+\nu}{1-\nu}\varepsilon^{00} \ (inside) \quad \varepsilon_r = -\frac{2}{3}\frac{1+\nu}{1-\nu}\frac{a^3}{r^3}\varepsilon^{00}, \ \varepsilon_t = \frac{1}{3}\frac{1+\nu}{1-\nu}\frac{a^3}{r^3}\varepsilon^{00} \ (outside)$$

Deviatoric stress is large near the interface outside the inclusion!

State of the Art

Phase-field models for plasticity:

- Proposed by X. Guo, S. Shi and X. Ma (2005)
  1) Assumed elastic-perfect plasticity – no hardening behavior
  2) Solves plastic strain by calculating the variation of deviatoric strain energy

Can the deviatoric strain energy be expressed as $E^{dis} = E^{dis}(e^{0}_{ij}, \varepsilon^{p}_{ij})$?

($e^{0}_{ij} = \varepsilon^{0}_{ij} - \varepsilon^{0}_{kk}\delta_{ij}/3$ is the deviatoric

Considering the solution of classical elastic in
spherical inclusion with dilatational eigenstrai

$\varepsilon_r = \varepsilon_t = \frac{1}{3}\frac{1+\nu}{1-\nu}\varepsilon^{00}$ (*inside*) $\varepsilon_r = -\frac{2}{3}\frac{1+\nu}{1-\nu}\frac{a^3}{r^3}$

Deviatoric stress is large near the interface ou

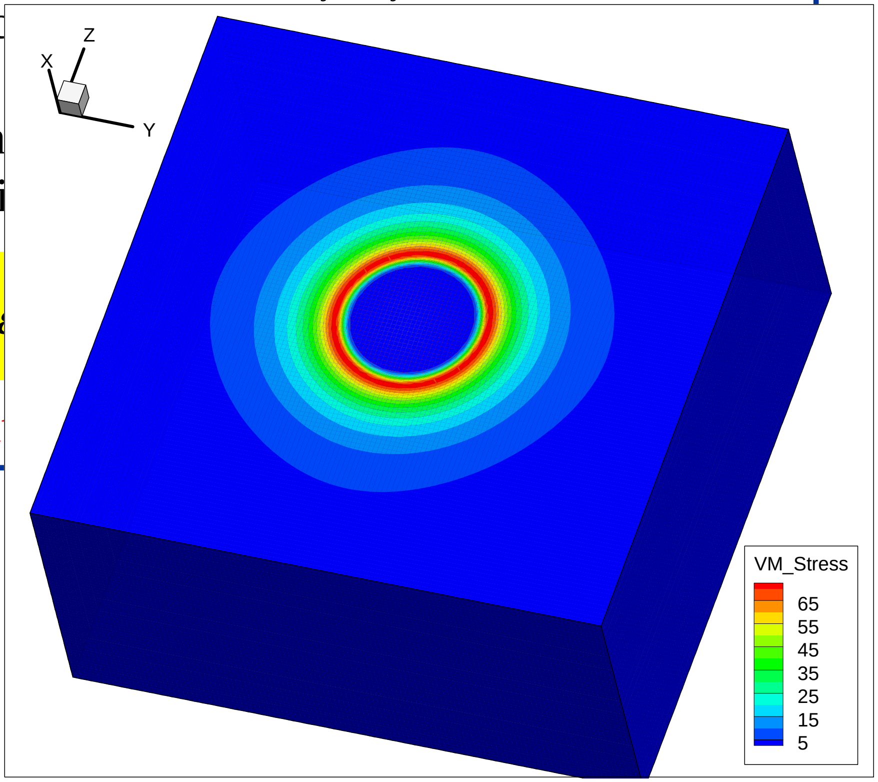

Need a thermodynamically consistent phase-field model for plasticity

A New Phase-Field Plasticity Model: Preliminary Results: Spherical Dilatational Inclusion in an Infinite Elasto-Perfect Plastic Matrix

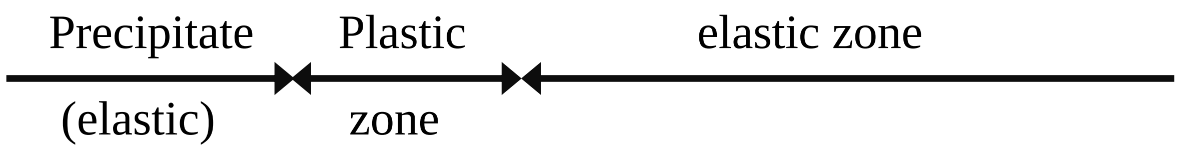

3% isotropic volume change is assumed in the inclusion.

SameYoung’s modulus and Poisson’s Ratio for matrix and inclusion. Yield strength for the matrix is set to be 1/10 of the inclusion.

Good agreement with analytical solution in stress components and plastic zone size

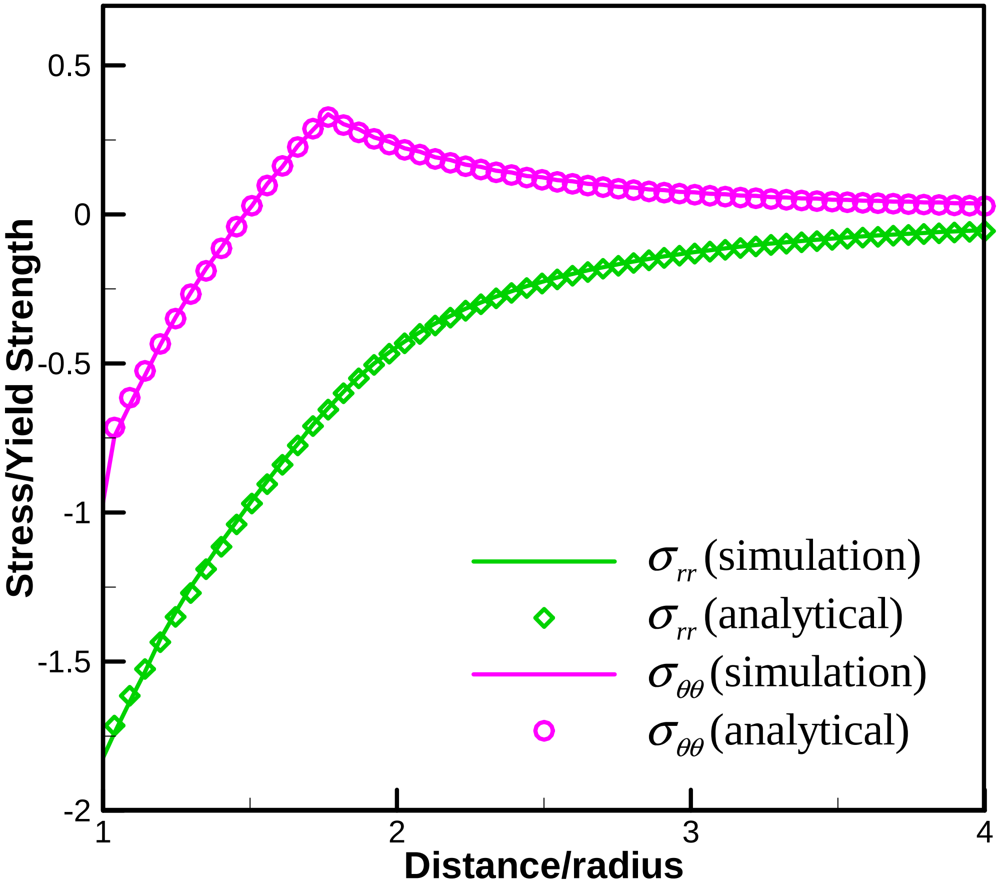

Analytical solution by J. Lee, Y. Earmme, H. Aaronson, K. Russell 1980

Preliminary Results: Prediction of coherent to incoherent transition based on energetics

$$\varepsilon_{ij}^{0} = \begin{bmatrix} 0.02 & & \\ & -0.01 & \\ & & -0.01 \end{bmatrix}$$

Pure deviatoric eigenstrain

$$\Delta G \sim 4\mu\delta^{2} \cdot \frac{4\pi r^{3}}{3} + 4\pi r^{2} \cdot \gamma$$

Porter & Easterling's model

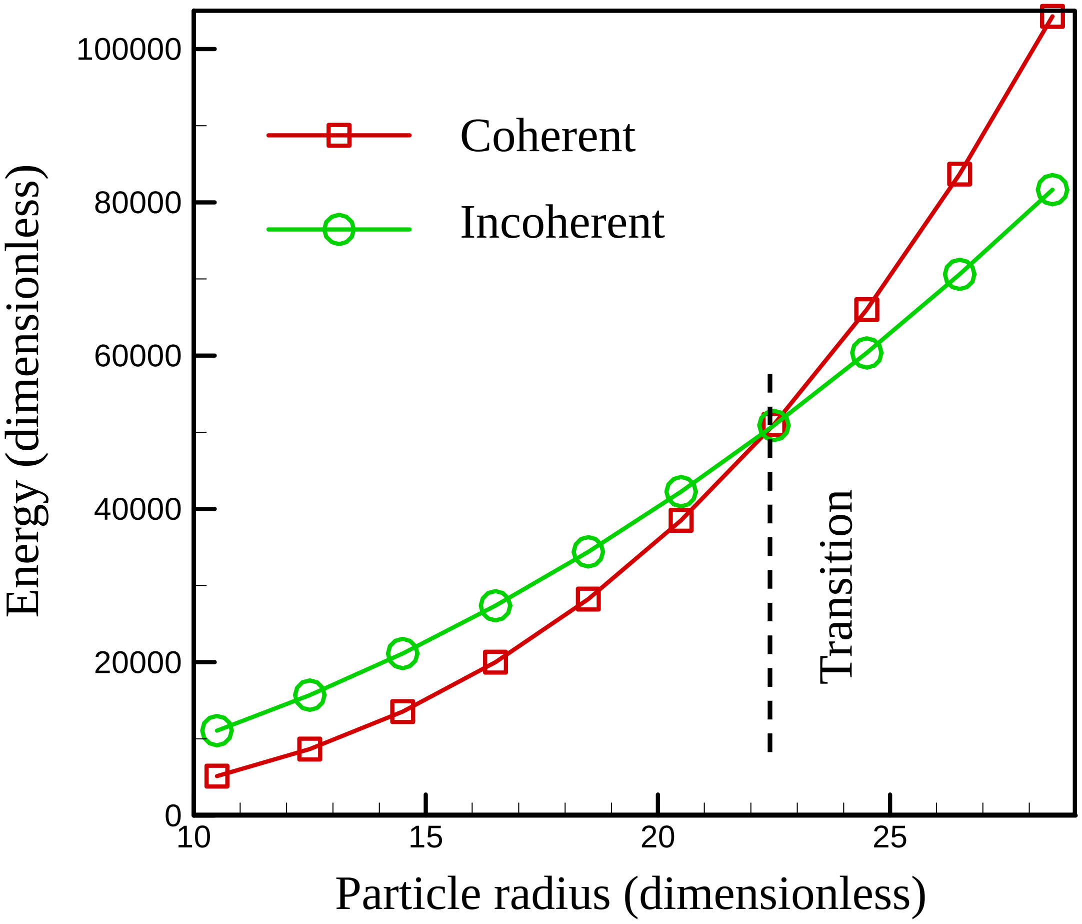

Preliminary Results: Coherent precipitate with both dilatational and deviatoric eigenstrain

$$\varepsilon_{ij}^{0} = \begin{bmatrix} 0.03 & & \\ & 0 & \\ & & 0 \end{bmatrix} = \begin{bmatrix} 0.01 & & \\ & 0.01 & \\ & & 0.01 \end{bmatrix} + \begin{bmatrix} 0.02 & & \\ & -0.01 & \\ & & -0.01 \end{bmatrix}$$

Dilatational + deviatoric

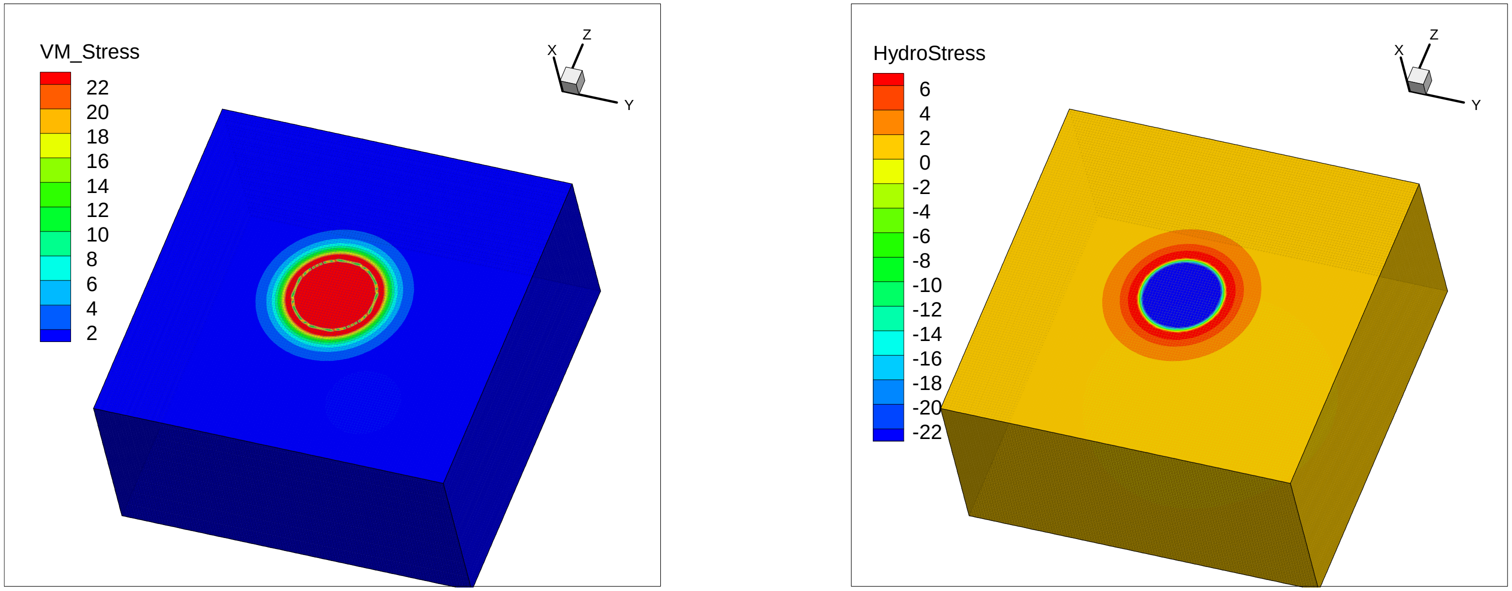

Von Mises stress and hydrostatic stress distribution with a coherent interface

Preliminary Results: Incoherent precipitate with both dilatational and deviatoric eigenstrain

$$\varepsilon_{ij}^{0} = \begin{bmatrix} 0.03 & & \\ & 0 & \\ & & 0 \end{bmatrix} = \begin{bmatrix} 0.01 & & \\ & 0.01 & \\ & & 0.01 \end{bmatrix} + \begin{bmatrix} 0.02 & & \\ & -0.01 & \\ & & -0.01 \end{bmatrix}$$

Von Mises stress and hydrostatic stress distribution with an incoherent interface: hydrostatic stress could not be completely removed in the precipitate!

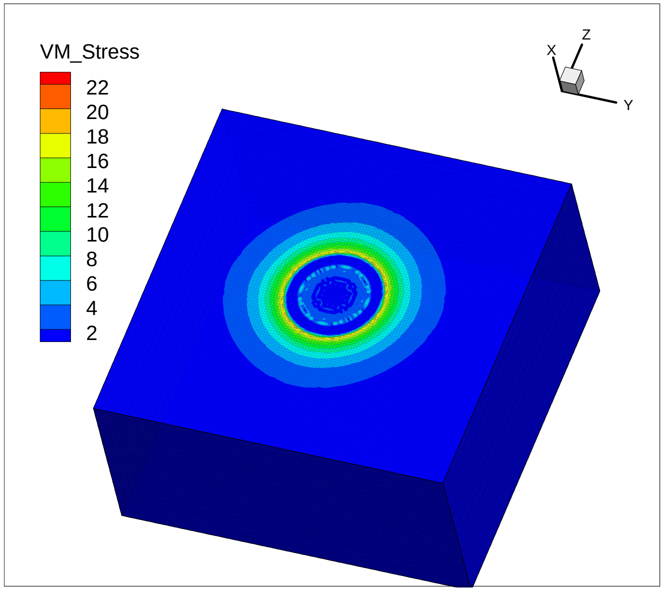

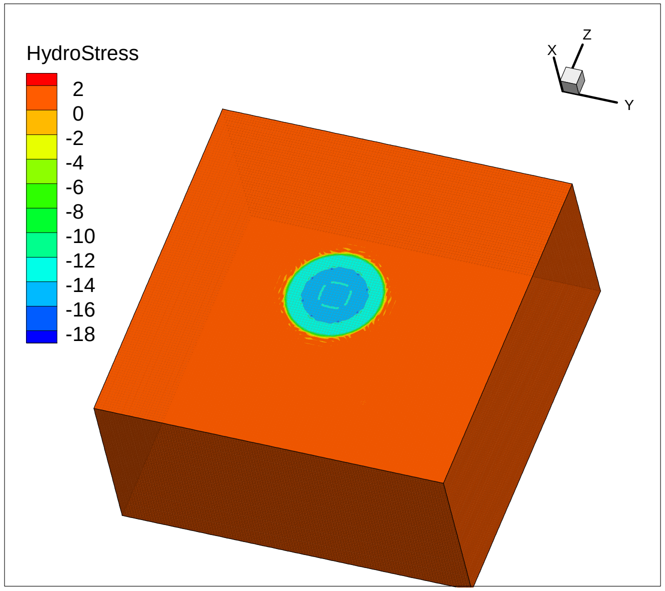

Porter and Eastering’s model needs to be reconsidered as they assumed elastic strain energy can be completely removed after loss of coherency.

Summary and Outlook

- **Developed a *simulation capability* based on Phase-Field Method to simulate external oxidation in simple systems**
- ***Further development* is on-going to develop an internal oxidation modeling capability that will eventually be able to simulate the transition from internal to external oxidation**